Journal of Chromatography A, 1217 (2010) 4704–4712

Contents lists available at ScienceDirect

Journal of Chromatography A

journal homepage: www.elsevier.com/locate/chroma

Modeling of thermal processes in very high pressure liquid chromatography for column immersed in a water bath: Application of the selected models

Joanna Kostka[a], Fabrice Gritti[b,c], Georges Guiochon[b,c], Krzysztof Kaczmarski[a,*]

[a] Department of Chemical and Process Engineering, Rzeszów University of Technology, 35-959 Rzeszów, Poland
[b] Department of Chemistry, The University of Tennessee, Knoxville, TN 37996-1600, USA
[c] Division of Chemical Sciences, Oak Ridge National Laboratory, Oak Ridge, TN 37831, USA

ARTICLE INFO

Article history:
Received 16 March 2010
Received in revised form 3 May 2010
Accepted 7 May 2010
Available online 19 May 2010

Keywords:
VHPLC
Heat generation
Viscous friction
Peak profiles
Equilibrium-dispersive model
Transport-dispersive model
POR model
Column efficiency

ABSTRACT

Currently, chromatographic analyses are carried out by operating columns packed with sub-2 μm particles under very high pressure gradients, up to 1200 bar for 5 cm long columns. This provides the high flow rates that are necessary for the achievement of high column efficiencies and short analysis times. However, operating columns at high flow rates under such high pressure gradients generate a large amount of heat due to the viscous friction of the mobile phase stream that percolates through a low permeability bed. The evacuation of this heat causes the formation of significant or even large axial and radial gradients of all the physico-chemical parameters characterizing the packing material and the mobile phase, eventually resulting in a loss of column efficiency. We previously developed and successfully applied a model combining the heat and the mass balances of a chromatographic column operated under very high pressure gradients (VHPLC). The use of this model requires accurate estimates of the dispersion coefficients at each applied mobile phase velocity. This work reports on a modification of the mass balance model such that only one measurement is now necessary to accurately predict elution peak profiles in a wide range of mobile phase velocities. The conditions under which the simple equilibrium-dispersive (ED) and transport-dispersive (TD) models are applicable in VHPLC are also discussed. This work proves that the new combination of the heat transfer and the ED model discussed in this work enables the calculation of accurate profiles for peaks eluted under extreme conditions, like when the column is thermostated in a water bath.

1. Introduction

Analysts in the pharmaceutical and fine chemical industries are under strong pressure to increase considerably the speed and throughput of HPLC analyses while keeping constant or even increasing peak resolutions. For these reasons, manufacturers of packing materials are preparing and packing new brands of finer silica particles. Various types of columns packed with sub-2 μm particles are now commercially available. The permeability of these columns is much lower than that of conventional columns but the velocity under which they should be operated for optimum results is larger. In order to fully exploit the potential of these new columns, analysts need to operate them under high inlet pressures, up to 1000 bar or more. However, high linear velocities of the mobile phase require steep pressure gradients along the columns and these combine to generate important amounts of heat. This heat, due to the friction of the mobile phase against the bed through which it percolates, escapes through axial convection, radial and axial conduction. This evacuation causes an important thermal heterogeneity of the column and losses of its efficiency that depend on the thermal environment of the column.

An abundant literature [1–19] deals with theoretical and experimental investigations of the consequences of heat generation by viscous friction in chromatographic columns: (1) the degree of thermal heterogeneity due to the evacuation of this heat; (2) the distributions throughout the columns of the temperature, hence the mobile phase velocity, the viscosity and the density, and (3) the resulting column efficiency. Recently, the profiles of peaks eluted from a column immersed in a water bath were determined in a wide range of mobile phase flow rates and at several bath temperatures [20]. It was shown that, when the temperature of the column wall is kept constant, the peak profiles are Gaussian at low flow rates and become trapezoidal at high flow rates (i.e., at very high inlet pressures).

We previously [21,22] described a new model accounting for column behavior under such conditions. This model combines the heat balance of the column and its mass balance in the equilibrium-

* Corresponding author. Tel.: +48 17 865 12 95; fax: +48 17 854 36 55.
E-mail addresses: kkaczmarski@prz.edu.pl, kkaczmarski@prz.rzeszow.pl (K. Kaczmarski).

0021-9673/$ – see front matter © 2010 Elsevier B.V. All rights reserved.
doi:10.1016/j.chroma.2010.05.018

Nomenclature

C	concentration in mobile phase
$\overline{C_p}$	average concentration in the mobile phase
d_p	adsorbent diameter
D_{eff}	effective particle diffusivity
$D_{z,a}$	axial apparent dispersion coefficient
D_L	axial dispersion coefficients
$D_{r,a}$	radial apparent dispersion coefficient
D_m	molecular diffusion coefficient
E	activation energy
F	phase ratio
F_v	volumetric mobile phase flow
H	Henry constant
k	overall mass transfer coefficient
k_{ext}	external mass transfer coefficient
k_f	apparent overall mass transfer coefficient
L	column length
N	number of theoretical plates
q	concentration in stationary phase
q^*	equilibrium concentration in solid phase
q_s	saturation capacity
$\bar{q}$	average concentration in stationary phase
R	gas constant
R_p	the particle radius
t	time
t_p	injection time
T	temperature
u	superficial velocity
V_m	partial molar volume
w	interstitial velocity

Greek symbol

ε_e	external porosity
ε_t	total column porosity
ε_p	particle porosity
γ_1, γ_2	geometrical constant
η	viscosity
ρ	density
τ	tortousity parameter

Subscripts

F	inlet value
ext	external

dispersive (ED) model with an isotherm model for the analyte, and the equations accounting for flow in porous media. It takes into account the influence of the axial and radial distributions of the local temperature and pressure on the values of the viscosity and density of the mobile phase, on its velocity, and on the Henry constant of the analyte. This model was validated by its correct predictions of the temperature distribution along the walls of columns packed with either conventional 5 μm particles or sub-2 μm particles, and of elution band profiles of analytes. Noteworthy were the correct predictions of peak profiles eluted from a sub-2 μm particle column held in a water bath at 299 K. This good agreement between calculated and recorded peak profiles was achieved, however, only because the apparent axial dispersion coefficient needed in the ED model was estimated separately, by parameter identification, at each mobile phase velocity studied.

The efficiency of columns operated under VHPLC conditions at constant wall temperature can be extremely low, as low as a few hundred theoretical plates. At such low efficiencies, the solution of the classical ED or TD models may differ considerably from that given by the general rate (GR) or the lumped pore diffusion model (POR). We previously proposed [23,24] the use of correlations between the apparent dispersion coefficient (for the ED model) or the effective overall mass transfer coefficient (for the TD model) and proved that these models could be applied to predict the profiles of bands eluted from very low efficiency columns. However, the applicability of these correlations has never been checked yet for chromatographic systems in which the physico-chemical parameters vary along and across the column because this column is thermally heterogeneous.

The goals of this work are: (1) a discussion of the conditions of applicability of the simple equilibrium-dispersive (ED) and transport-dispersive (TD) models under VHPLC conditions; (2) a presentation of a modified mass balance model enabling the prediction of the elution profiles of solutes in a wide range of mobile phase velocities based on the measurement of a single kinetic parameter requiring only one experiment; and (3) the validation of the proposed model for columns operated at different wall temperatures.

To validate the proposed model, we chose the experimental conditions that are the most unfavorable and difficult for this modeling, the thermal environment in which the chromatographic column is immersed in a liquid bath with a fast, turbulent water flow. Under such conditions, the column wall temperature is kept constant, equal to the water temperature, due to the very high external heat transfer between the column wall and the water in the bath. On other hand and due to the radial heat flux, a steep radial temperature gradient, hence steep radial gradients of mobile phase velocity, viscosity, and density, and of retention factors form across the column. Shallow axial gradients of all these parameters also are formed. If the model is validated under such conditions, it should also correctly predict the column behavior under the less severe conditions that are typically chosen in laboratory practice, with the column operated in a closed, still air bath.

2. Mathematical models

The mathematical model developed to account for the consequences of the heat generated in the column by the friction of the mobile phase percolating through the bed consists in the fusion of three separate models: (1) a model of heat transfer; (2) a model of mobile phase velocity distribution; and (3) a model of mass transfer. The first of these models expresses how heat is generated by viscous friction and how it is evacuated from the column under steady-state conditions. The boundary conditions for this model assume a constant wall temperature equal to that of the temperature-controlled water bath. The second model accounts for the distribution of mobile phase velocities across the column, which depend on the local temperature and pressure provided by the first model and on the equations of hydrodynamics in porous media. These two models are exactly the same as those described in our previous paper [22] and need not be described again. To solve these two models, we need the eluent density, viscosity, thermal expansion coefficient, and heat capacity as a function of pressure and temperature. These values and the effective thermal conductivity of the bed were calculated using the correlations given in [22].

The third model accounts for the propagation of a compound band along a column that is no longer isothermal. Then, the equilibrium constant depends on the local temperature and pressure; so does the migration velocity of a concentration. In this work we applied a modified equilibrium-dispersive (ED), a transport-dispersive (TD), and the lumped pore diffusion model (POR) [23,24].

2.1. The mass balance equations

Numerous mathematical models are available to account for the band profiles obtained in chromatography [25]. The most sophisticated and exact model is the general rate model (GR). When the mass transfer resistances inside the adsorbent particles are moderate, the POR model can be applied. When the overall mass transfer resistances are small and have but a minor influence on band profiles, the ED model is recommended.

In earlier papers [23,24] it was proven that even the ED or the TD models could be applied to low efficiency columns provided that the apparent dispersion coefficient (in the ED model) or the effective overall mass transfer coefficient (in the TD model) are calculated from an appropriate correlation (see next section, Eqs. (10) and (14)). In such a case, the peak profiles calculated with the ED or the TD model are identical or almost identical to those given by the GR or the POR model. Eqs. (10) and (14) were developed to be applied under linear conditions, meaning at constant mobile phase velocity and constant value of the isotherm Henry constant throughout the whole column. In this work, we must check whether these equations can also be applied when the Henry constant depends on the position in column (due to the temperature and pressure distributions) and when both a radial and an axial gradient of mobile phase velocity exist everywhere. The test of consistency of the results of the POR, ED and TD models will be performed also for nonlinear isotherms (nonlinear dependency of q on C).

2.1.1. POR model

The most sophisticated model of mass transfer used in this work is the lumped pore diffusion model. In a cylindrical system of coordinates, the mass balance equation for the mobile phase is written as follows [23]:

$$\frac{\delta C}{\delta t} + \frac{u_z}{\varepsilon_e}\frac{\delta C}{\delta z} + \frac{C}{\varepsilon_e}\,\mathrm{div}(\mathbf{u}) = D_L\frac{\delta^2 C}{\delta z^2} + D_{r,\alpha}\left(\frac{1}{r}\frac{\delta C}{\delta r} + \frac{\delta^2 C}{\delta r^2}\right) - \frac{1-\varepsilon_e}{\varepsilon_e}k\frac{6}{d_p}(C-\overline{C_p}) \quad (1)$$

This equation was obtained by adding dispersion in the radial direction to the classical equation of the unidimensional POR model.

The mass balance of the solute in the mobile phase impregnating the adsorbent pores is

$$\varepsilon_p\frac{\delta\overline{C_p}}{\delta t} + (1-\varepsilon_p)\frac{\delta\bar{q}}{\delta t} = k\frac{6}{d_p}(C-\overline{C_p}) \quad (2)$$

where C is the analyte concentration in the mobile phase (g/l), $\overline{C_p}$ and $\bar{q}$ are its average concentrations in the mobile and the stationary phases (g/l), D_L and $D_{r,a}$ are the average axial dispersion and average radial apparent dispersion coefficients (m^2/s), respectively, u_z (m/s) is the superficial velocity, r and z are the radial and axial coordinates respectively, ε_e, ε_p are the external bed and particle porosities respectively, t is the time (s), d_p is the particle diameter (m) and k is the overall mass transfer coefficient (m/s).

In this work, we neglect the radial convective term in Eq. (1) because the mobile phase velocity in the radial direction is negligible compared to the axial velocity [21]. For the same reason, div($\mathbf{u}$) was approximated by $\delta u_z/\delta z$ in all three models. In our previous papers [21,22] the term containing div($\mathbf{u}$) was neglected. Neglecting this term in the high pressure range, however, may cause an error of a few percent in the mass balance.

The sets of equations of the models 1 and 2 were solved with the following initial and boundary conditions:

- Initial conditions, for $t = 0$

$$C(0,z,r) = 0\overline{C_p}(0) = \bar{q}(0) = 0 \quad (3)$$

- Boundary conditions for Eq. (1).
  for $t > 0$; $z = 0$

$$u_F C_F^0 - u(0)C(0) = -\varepsilon_e D_L\frac{\delta C}{\delta Z};\quad C_F^0 = \begin{cases} C_F & \text{for } 0 < t < t_p \\ 0 & \text{for } t < t_p \end{cases} \quad (4)$$

  for $t > 0$; $z = L$;

$$\frac{\delta C}{\delta z} = 0 \quad (5)$$

For $t > 0$, $r = R_p$ and $r = 0$:

$$\frac{\delta C}{\delta r} = 0 \quad (6)$$

where t_p is the injection time (s), R_p is the particle radius (m), and subscript F denotes the inlet value.

The overall mass transfer coefficient, k, is a function of the external mass transfer coefficient, k_{ext}, and the effective particle diffusivity, D_{eff}:

$$k = \left[\frac{1}{k_{ext}} + \frac{d_p}{10D_{eff}}\right]^{-1} \quad (7)$$

The effective particle diffusivity is evaluated from the following relationship:

$$D_{eff} = \frac{\varepsilon_p D_m}{\tau} \quad (8)$$

where d_p is the particle diameter (m), τ is a tortuosity parameter, and D_m is the diffusion coefficient (m^2/s).

2.1.2. ED model

The mass balance equation of the ED model is written as follows [21]:

$$\frac{\delta C}{\delta t} + F\frac{\delta q}{\delta t} + \frac{\delta(w_z C)}{\delta z} = D_{Z,\alpha}\frac{\delta^2 C}{\delta z^2} + D_{r,a}\left(\frac{1}{r}\frac{\delta C}{\delta r} + \frac{\delta^2 C}{\delta r^2}\right) \quad (9)$$

where C and q are the analyte concentrations in the mobile and in the stationary phases (g/l), respectively, $D_{z,a}$ and $D_{r,a}$ are the average axial and radial apparent dispersion coefficients (m^2/s), respectively, $w_z = u_z/\varepsilon_t$ (m/s) is the interstitial velocity, $F = (1-\varepsilon_t)/\varepsilon_t$ is the phase ratio and ε_t is the total porosity of the column.

In earlier papers [23,24], it was proved that the solution of the unidimensional ED model (without a radial term but with a constant mobile phase velocity) is compatible with the GR or the POR model when the axial apparent dispersion coefficient is calculated from the following equation:

$$D_{z,a} = \frac{D_L\varepsilon_e}{\varepsilon_t} + \left(\frac{k_1}{1+k_1}\right)^2\frac{u^2 d_p}{\varepsilon_t\varepsilon_e F_e 6}\left[\frac{d_p}{10D_{eff}} + \frac{1}{k_{ext}}\right] \quad (10)$$

where

$$k_1 = F_e\left(\varepsilon_p + (1-\varepsilon_p)\frac{\delta q}{\delta C}\right);\quad F_e = \frac{1-\varepsilon_e}{\varepsilon_e} \quad (11)$$

In this work the apparent axial dispersion coefficient $D_{z,a}$ was calculated from Eq. (10).

The initial and boundary conditions are similar to those used for the POR model.

2.1.3. TD model

The TD model in the form compatible with the GR model is written as follows [23]:

$$\frac{\delta C}{\delta t} + F\frac{\delta q}{\delta t} + \frac{\delta(w_z C)}{\delta z} = \frac{\varepsilon_e}{\varepsilon_t} D_L \frac{\delta^2 C}{\delta z^2} + D_{r,a}\left(\frac{1}{r}\frac{\delta C}{\delta r} + \frac{\delta^2 C}{\delta r^2}\right) \quad (12)$$

where a term for dispersion in the radial direction was added to the classical equation of the unidimensional TD model. The TD model is then completed with the following kinetic equation:

$$\frac{\delta q}{\delta t} = k_f(q^* - q) \quad (13)$$

where the parameter k_f is the apparent overall mass transfer coefficient [m/s] and q^* is the equilibrium concentration in the solid phase corresponding to the concentration C in the mobile phase. The apparent overall mass transfer coefficient is calculated from the formula [24]:

$$k_f = \frac{F_e k \varepsilon_e 6}{d_p \varepsilon_t k'_o}\left(\frac{k'_o(1+k_1)}{k_1(1+k'_o)}\right)^2 \quad (14)$$

where

$$k'_o = \frac{1-\varepsilon_t}{\varepsilon_t}\frac{\delta q}{\delta C} \quad (15)$$

The initial and boundary conditions are similar to those for the POR model.

2.1.4. Isotherm equation

Models ED, TD and POR must be combined with an appropriate isotherm equation for the solute. In this work, we consider a linear isotherm:

$$q = H \cdot C \quad (16)$$

where H is the Henry constant. In a linear isotherm, H does not depend on the concentration. However, H is a function of the temperature and the pressure [25]:

$$H = H_0 \cdot \exp\left(-\frac{E}{RT}\right) \cdot \exp\left(-\Delta V_m \frac{P - P_{ref}}{RT}\right) \quad (17)$$

where E is the activation energy of adsorption, R is the universal gas constant and ΔV_m is the difference between the partial molar volumes of the solute in the adsorbed layer and in the liquid phase.

Besides the linear isotherm, the Langmuir isotherm was also considered, with:

$$q = \frac{H \cdot C}{1 + (H/q_S) \cdot C} \quad (18)$$

2.2. Methods of calculation of the physico-chemical parameters for the mass balance equations

To solve the mass balance equations discussed above, the external mass transfer coefficient, k_{ext}, the dispersion coefficient D_L, the radial apparent dispersion coefficient, $D_{a,r}$, the molecular diffusivity, D_m, and the tortuosity parameter, τ, must be calculated.

In the literature, the correlations most frequently recommended for the calculations of the external mass transfer coefficient are the equations elaborated by Pfeffer [26], Wilson and Geankoplis [27], and Kataoka et al. [28]. The applicability of these formulas under chromatographic conditions was recently confirmed by Miyabe et al. [29]. In this work we calculated k_{ext} from the Wilson and Geankoplis correlation which gives:

$$Sh = \frac{1.09}{\varepsilon_e} Re^{0.33} Sc^{0.33} \quad (19)$$

where

$$Sh = \frac{k_{ext} d_p}{D_m} \quad Re = \frac{u d_p \rho}{\eta} \quad Sc = \frac{\eta}{\rho D_m}$$

The dispersion coefficient can be calculated from the Gunn [30] or the Wen and Fan correlations [31]. Another method is to approximate the dispersion coefficient by the relationship [25]:

$$D_L = \gamma_1 D_m + \gamma_2 u d_p \quad (20)$$

where γ_1 and γ_2 are geometrical constants. It was assumed that $\gamma_1 = 0.7$ [25] whereas γ_2 was estimated from the experimental data.

The molecular diffusion coefficient D_m was estimated from the Scheibel [32] equation, often recommended in the literature [25,33]:

$$D_m = D_{A,B} = \frac{AT}{\eta_B V_A^{1/3}}\left[1 + \left(\frac{3BV_B}{V_A}\right)^{2/3}\right] \quad (21)$$

where V_A and V_B are a molar volumes of the solvent and the solute, respectively, and A is a constant, the value of which depends on ratio of V_A to V_B [25].

To solve the mass balance equation, the apparent radial dispersion coefficients are also needed. The radial dispersion coefficient, $D_{a,r}$, was calculated on the basis of the plate height equation derived by Knox [34,35,22]:

$$D_{a,r} = \frac{0.03 d_p u}{\varepsilon_t} + 0.7 D_m \quad (22)$$

The tortuosity parameter, τ, was calculated from the correlation [25]:

$$\tau = \frac{(2-\varepsilon_p)^2}{\varepsilon_p} \quad (23)$$

2.3. Method of calculation of numerical solutions of the models

The coupled mass balance and heat balance equations were solved with a method previously described in details in [21,22]. First, the steady-state distributions of the temperature and the pressure throughout the column were derived. Afterwards, the time dependent mass balance equation was solved, using the temperature and the pressure profiles previously obtained. The heat balance and the differential mass balance equations were solved using the method of orthogonal collocation on finite elements (OCFE) in its analog version previously described [36]. The spatial derivatives were discretized, following the OCFE method. The set of ordinary differential equations obtained through this process was then solved using the VODE solver [37].

3. Experimental

The experiments and their results were described in details in an earlier paper [20]. Among these results, those obtained with the column kept in a temperature-controlled water bath are analyzed in this paper. In the following section, we briefly describe the experimental conditions.

3.1. Chemical

A 85/15 (v/v) aqueous solution of acetonitrile was used as the mobile phase. HPLC grade acetonitrile was purchased from Fisher Scientific (Fair Lawn, NJ, USA). Dichloromethane and tetrahydrofuran (also from Fisher Scientific), both HPLC grade, were used to determine the hold-up volumes of the columns, using the pycnometric method [38]. The solvents were filtered before use on an SFCA filter membrane, 0.2 μm pore size (Suwannee, GA, USA). Eleven polystyrene standards were used to acquire the ISEC data

needed to estimate the column porosities (MW 590, 590, 1100, 3680, 6400, 13 200, 31 600, 90 000, 171 000, 560 900, 900 000, and 1 860 000). They were purchased from Phenomenex (Torrance, CA, USA). Naphtho[2,3-α]pyrene was used as the solute and was purchased from Fisher Scientific.

3.2. Materials

3.2.1. Columns

The 2.1 × 50 (I.D. (mm) × L (mm)) column used in this study was from Waters (Mildford, MA, USA). It was packed with 1.7 μm particles of bridged ethylsiloxane/silica-C18 packing material (BEH). The characteristics of the adsorbent particles are average pore diameter—130 Å, specific surface area—185 m^2/g, bonded phase—endcapped BEH-C18, total carbon—18%, surface coverage—3.1 μmol/m^2. The total porosity of the bed was 0.642, the external porosity 0.373, and the particle porosity 0.429.

3.3. Apparatus

The column was operated with an Acquity UPLC liquid chromatograph (Waters, Milford, MA, USA). This instrument includes a quaternary solvent delivery system, an autosampler with a 10 μl sample loop, a monochromatic UV detector, a column thermostat, and a data station running the Empower data software from Waters.

From the exit of the Rheodyne injection valve to the column inlet and from the column outlet to the detector cell, the total extra-column volume of the instrument is 13.5 μl, as measured by replacing the column with a zero-volume union connector. The flow rate delivered by the high-pressure pumps of the instrument is true at the column inlet. The flow rate eventually measured at the column outlet depends on the inlet pressure and on the eluent compressibility. The maximum pressure that the pumps can deliver is 1034 bar. The maximum flow rate is 2.0 ml/min. All measurements were carried out with the column immersed in a thermostated water bath.

The column was connected to the pump using a 25 cm long steel tube, with an internal diameter of 0.127 mm. This connecting tube was immersed in the water bath. Under such conditions and for any mobile phase velocity applied in this work, the fluid temperature at the column inlet was equal to that of the water bath.

4. Results and discussion

For column inlet pressures below ca. 100 bar, the heat generated by viscous friction is small, the column is isothermal and all the column physico-chemical parameters can be regarded as constant. In contrast, for an inlet pressure of 1000 bar, the difference between the column inlet and outlet temperatures may exceed 20 °C and the difference between the temperatures in the column center and near its wall, at a distance of only 1 mm, may reach 5 °C. Such an important radial temperature gradient causes a considerable reduction of the column efficiency [22]. The radial thermal gradient is smallest when the column is operated under natural convective conditions and the radial heat losses are moderate. This gradient is largest when the column is immersed in a water bath with a strong circulation of thermostated water, and fast convective heat transfer keep constant the column wall temperature. We previously proved [22] that the heat transfer model coupled with the simple ED mass transfer model as we proposed accurately predicts the peak profiles of naphtho[2,3-α]pyrene for column inlet pressures up to 1000 bar, when the water bath temperature is 299 K. However, an excellent agreement is achieved between the calculated and the experimental elution profiles only if the axial dispersion coefficient is estimated for each mobile phase velocity.

In this work, we report on tests of the model described in the Theory section, which combines the heat transfer model and one of the mass transfer models, the POR, TD, or ED models. These tests were made in a wide range of experimental conditions, for water bath temperatures of 299, 310 and 329 K and for mobile phase flow rates between 0.03 and 1.8 ml/min. To solve these mass transfer models, the values of the external mass transfer coefficient, k_{ext}, and of the dispersion coefficients, D_L and $D_{a,r}$, were calculated from Eqs. (19), (20), and (22), using for these calculations the known physico-chemical conditions at the column inlet and outlet and their average values.

The isotherm model parameters, $H_o = 2.936 \times 10^{-4}$ and $E/R = 3245$, were derived from the measurements of the retention time of naphtho[2,3-α]pyrene at 299, 310 and 329 K, at a mobile phase velocity of 0.12 ml/min, at which the heat effects are negligible. The difference between the partial molar volumes of the solute in the adsorbed and the liquid phase, $\Delta V_m = -1.1 \times 10^{-5}$ m^3/mol, was derive from the results of the measurements of the peak retention time at a mobile phase velocity of 1.5 ml/min, with a water bath temperature of 299 K. These values of H_o and E/R were used for the calculation of the peak profiles at temperature $T = 299$ K. We found a better agreement between experimental and theoretical peak profiles if the calculations made for the temperatures of 310 and 329 K used the values of H_o and E/R derived from the measurements of the retention times of naphtho[2,3-α]pyrene at 310 and 329 K, giving $H_o = 8.242 \times 10^{-4}$ and $E/R = 2929$.

Comparison between the band profiles calculated with the ED, the TD, and the POR models under very high pressure gradients were also performed with a Langmuir isotherm, assuming an arbitrary value of the saturation capacity, $q_s = 50$ g/l, the other parameters remaining the same as for the linear isotherm. With a nonlinear isotherm, however, the ED model must be modified. The axial apparent dispersion term in Eq. (9), $D_{z,a}$, depends on the position along the column, due to its dependency on the solute concentration (see Eqs. (10) and (11)). So, the model must be replaced by:

$$\frac{\delta C}{\delta t} + F\frac{\delta q}{\delta t} + \frac{\delta (w_z C)}{\delta z} = \frac{\delta}{\delta z}\left(D_{z,a}\frac{\delta C}{\delta z}\right) + D_{r,a}\left(\frac{1}{r}\frac{\delta C}{\delta r} + \frac{\delta^2 C}{\delta r^2}\right) \quad (9a)$$

4.1. Comparison of the results of the calculations made with the ED, the TD and the POR models

As stated above, the band profiles calculated with the ED and the TD models are consistent with those obtained with the GR and the POR models provided that the effective dispersion coefficient (in the ED model) or the effective overall mass transfer coefficient (in the TD model) are calculated from Eqs. (10) or (14), respectively [23,24]. The ED or TD models predict very well the peak profiles calculated with the GR or POR models, even for column efficiencies as low as a few theoretical plates. Eqs. (10) and (14) were developed for cases in which the isotherms are linear and the physico-chemical parameters of the system are constant throughout the whole column. It was proved later that these equations can also be applied in the cases in which the isotherms are nonlinear but it was not yet clear whether solutions of the simple ED and TD models can approach closely enough the solution obtained with the more sophisticated GR or POR models when the column is operated at high mobile phase velocity, under a very high pressure drop and is no longer isothermal. In such cases, the amount of heat generated by viscous friction is large, considerably affecting the distributions of the physico-chemical parameters of the system (retention constant, viscosity, density, mobile phase velocity, diffusivity) in both the radial and axial directions.

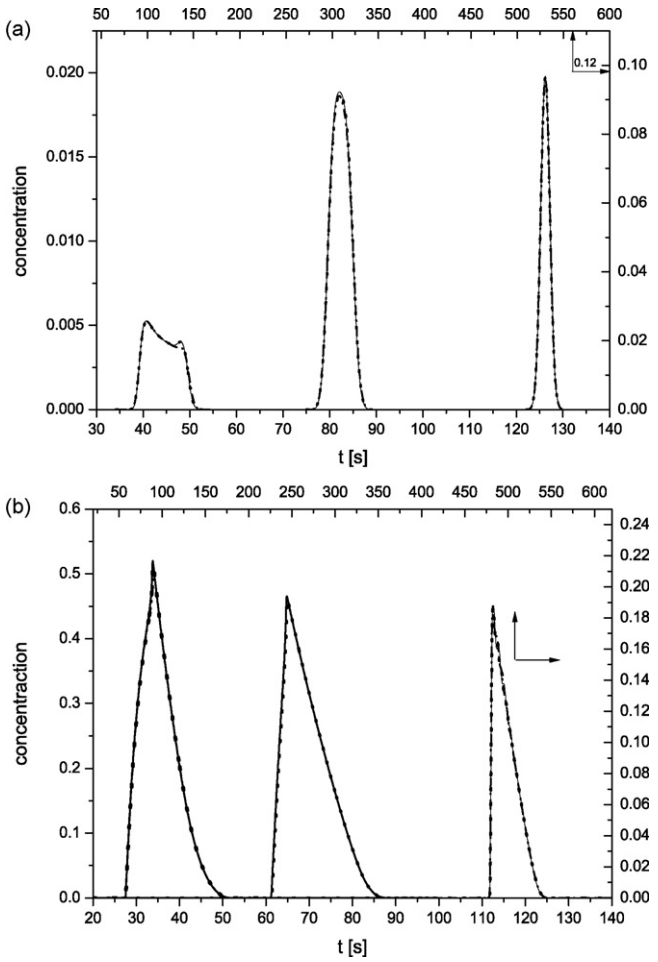

Fig. 1. Comparison between concentration profiles calculated with the ED, the TD, and the POR models. (a) Linear isotherm and (b) nonlinear isotherm. Column: 5 cm × 0.21 cm, wall temperature kept at 299 K. Solid line, ED model; dotted line, TD model; dash-dotted line, POR model. F_v = 1.5, 0.8, 0.12 ml/min (from left to right).

In this work we compared the numerical solutions provided by the ED and the TD models with those calculated using the POR model. The calculations were made for mobile phase flow rates of 0.12, 0.8, and 1.5 ml/min and for a water bath temperature of 299 K. Two series of calculation were made, one for the linear isotherm and the second for a nonlinear isotherm. The temperature distribution was calculated with the method described in Refs. [21,22]. The mass balances were calculated using these temperature distributions and the average values of the kinetic parameters: k_{ext}, D_L and $D_{a,r}$. The last unknown parameter, γ_2, in Eq. (20) was assumed to be equal to 1.62 (see next section).

The band profiles calculated for a linear isotherm are shown in Fig. 1a and those calculated for a nonlinear isotherm in Fig. 1b. For a linear isotherm and at the lowest mobile phase velocity, the elution peak has a nearly Gaussian profile, practically unaffected by the heat generation, whereas, at the largest velocity, the band profile resembles a trapezoid. Similarly, for a nonlinear isotherm, the elution peak has the classical triangular profile associated with the Langmuir isotherm whereas, at the largest velocity, the Langmuir peak profile is deformed and the shock layer has disappeared.

A more detailed comparison between experimental and theoretical peak profiles in linear chromatography is presented in the next section. A similar comparison for nonlinear chromatography will be presented later.

From the results of our calculations presented here, it follows that the numerical solutions obtained with the ED and the TD models agree very well with the solution of the POR model. However, the calculation time is shorter with the ED model. Depending on the physico-chemical conditions of the specific problem studied, the calculation times with the TD and with the POR models can be several times and one to two orders of magnitude larger than with the ED model, respectively.

The calculations discussed in the next section were done with ED model.

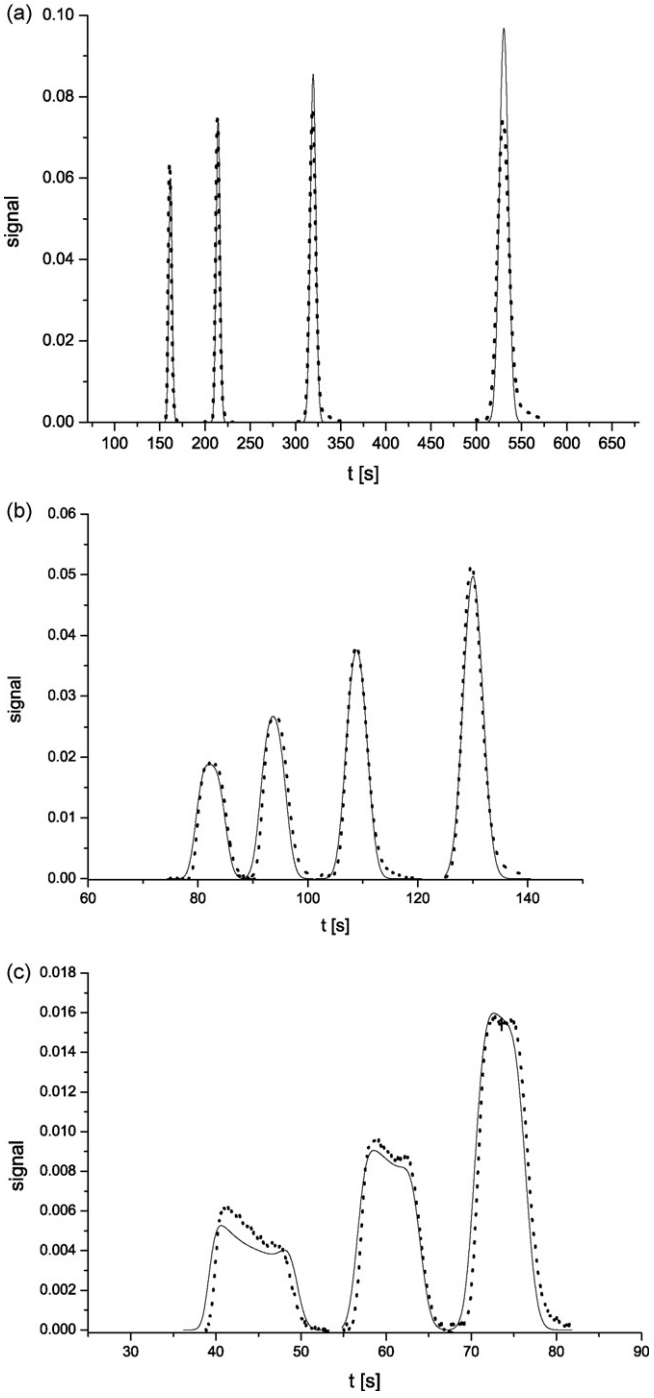

Fig. 2. Comparison between experimental (symbols) and theoretical (solid lines) concentration profiles of naphtho[2,3-α]pyrene. Column: 5 cm × 0.21 cm thermostated in a water bath at 299 K. F_v = 0.4, 0.3, 0.2, 0.12 ml/min (from left to right), with P = 210, 161, 114, 75 bar, respectively, F_v = 0.8, 0.7, 0.6, 0.5 ml/min (from left to right), with P = 419, 365, 313, 261 bar, respectively, F_v = 1.5, 1.1, 0.9 ml/min (from left to right) with P = 808, 580, 470 bar, respectively,

4.2. Comparison of experimental and theoretical peak profiles

In our previous work, we successfully used the simple ED model in Eq. (9) for the calculation of peak profiles eluted from a column thermostated in a water bath at 299 K. However, to obtain a good agreement between theoretical and experimental peak profiles, the value of the apparent dispersion coefficient at each mobile phase velocity used must be estimated from the corresponding experimental data, separately. As will be demonstrated in the following, this drawback can be overcome by calculating the axial apparent dispersion coefficient from Eq. (10) and all the other parameters but γ_2 from the correlations presented in Section 2.3. The value of the γ_2 parameter was estimated at each temperature studied, for the mobile phase velocity at which the van Deemter curve reaches its minimum. This corresponds to a value of F_v equal to approximately 0.3 ml/min [20]. The values obtained for γ_2 were 1.62, 3.38 and 4.40 at the temperatures of 299, 310 and 329 K, respectively.

A comparison between the experimental and the calculated peak profiles are shown in Figs. 2–4. At each temperature and for mobile phase flow rates greater than about $F_v = 0.2$ ml/min, the results of the calculations agree excellently with the experimental profiles. This result is important because flow rates larger than about 0.2 ml/min correspond to the most important flow rate range used in practical applications, the right branch of the van Deemter curve, in which it is recommended to perform chromatography separations.

In contrast, at mobile phase flow rates lower than 0.1 ml/min, the peak profiles calculated are always higher than those recorded. This discrepancy increases with decreasing fluid flow rate (data not presented). However, these flow rates correspond to the left branch of the van Deemter curve, a range that is generally considered as of minor importance in chromatographic analysis.

Besides the methods of calculation of elution band profiles presented earlier, we tested two other possible approaches:

1. The axial dispersion coefficient, D_L, was calculated from the Gunn and the Wen and Fan correlations.
2. The axial dispersion coefficient, D_L, was calculated as explained above but the effective dispersion coefficient D_{eff}, was estimated from the peak profile at one mobile phase velocity (in a fashion similar to that used to derive the value of γ_2).

In both cases, however, and in the whole range of mobile phase velocities investigated, the agreement between experimental and theoretical band profiles was generally much less good than it was for profiles calculated with the method presented above.

The loss of column efficiency is caused by the combined effects of (1) a radial distribution of the mobile phase viscosity, hence of the velocity; and (2) a radial distribution of the retention factor, k' (i.e., a radial Henry constant distribution). To compare the losses of column efficiency due to these two effects, we calculated the peak profiles at two mobile phase velocities, 1.5 and 0.8 ml/min, and at $T = 299$ K. In the first case, the inlet pressure was 808 bar, in the second it was 419 bar. The calculations were performed with three assumptions: (a) the full, correct model that takes into account the radial distributions of the Henry constant and the mobile phase velocity; (b) the Henry constant is independent of the temperature (with $T = 299$ K in Eq. (17)) but there is a radial distribution of the mobile phase velocity; and (c) the Henry constant and the mobile phase velocity are constant. The results obtained are presented in Fig. 5.

The first group of peaks was calculated for $F_v = 1.5$, the second for $F_v = 0.8$ ml/min. The highest peaks were all obtained for calculations made in assumption (c), the intermediate ones for calculations made in assumption (b) and the smallest ones for calculations made in assumption (a). The column efficiencies expressed in the numbers of theoretical plates, calculated with the method of moments, were as follows:

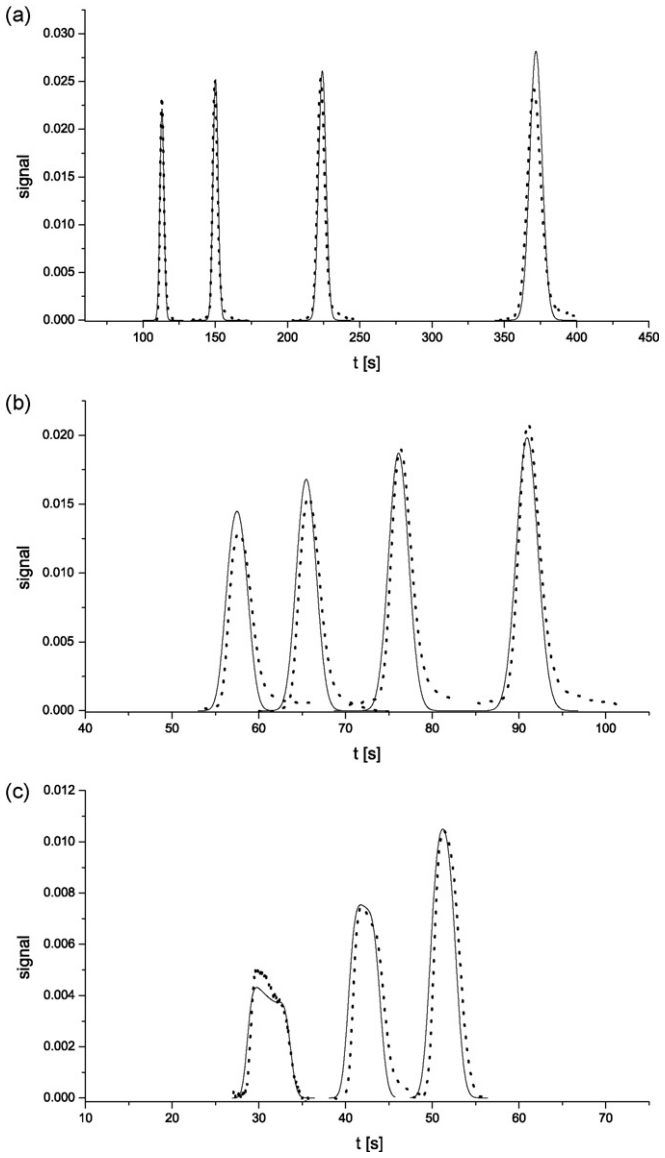

Fig. 3. Comparison between experimental (symbols) and theoretical (solid lines) concentration profiles of naphtho[2,3-α]pyrene. Column: 5 cm × 0.21 cm thermostated in a water bath at 310 K. $F_v = 0.4$, 0.3, 0.2, 0.12 ml/min (from left to right), with $P = 186$, 143, 100, 67 bar, respectively, $F_v = 0.8$, 0.7, 0.6, 0.5 ml/min (from left to right), with $P = 384$, 320, 274, 229 bar, respectively, $F_v = 1.5$, 1.1, 0.9 ml/min (from left to right), with $P = 703$, 504, 410 bar, respectively

At $F_v = 0.8$ ml/min, $N = 5661$, 4640 and 1922 in cases (c), (b) and (a), respectively.
At $F_v = 1.5$ ml/min, $N = 3366$, 1179 and 192, in cases (c), (b) and (a), respectively.

As seen in Fig. 5 and from the numbers of theoretical plates given above, the main source of loss of column efficiency in the case of naphtho[2,3-α]pyrene investigated here is the radial distribution of the retention factor, k'. The loss that is merely due to the radial distribution of the mobile phase velocity is important for a pressure drop of 800 bar. However, for inlet pressures lower than 400 bar, it becomes marginal.

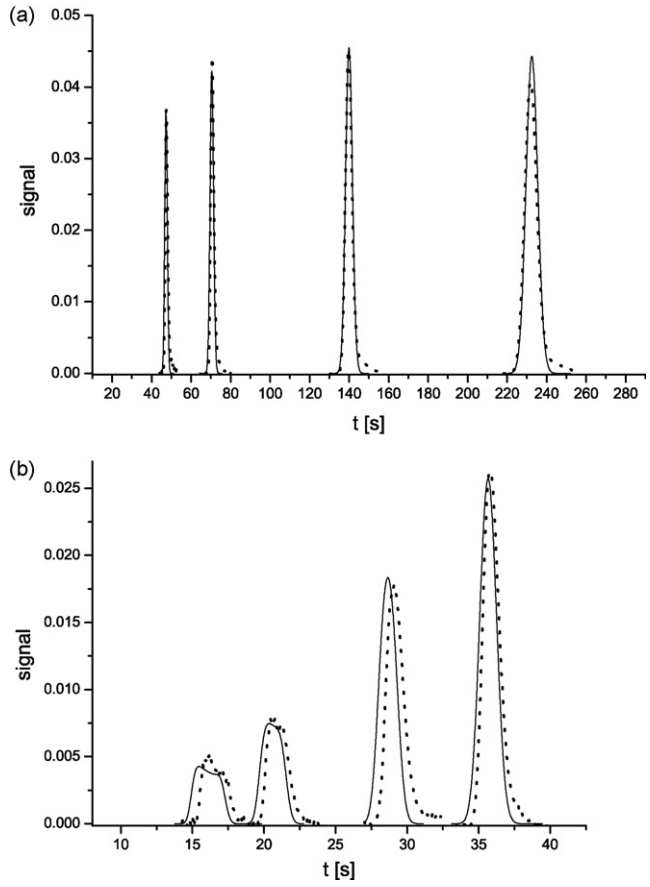

Fig. 4. Comparison between experimental (symbols) and theoretical (solid lines) concentration profiles of naphtho[2,3-α]pyrene. Column: 5 cm × 0.21 cm thermostated in a water bath at 329 K. F_v = 0.6, 0.4, 0.2, 0.12 ml/min (from left to right), with P = 226, 155, 86, 59 bar, respectively, F_v = 1.8., 1.4, 1.0, 0.8 ml/min (from left to right), with P = 694, 530, 375, 299 bar, respectively,

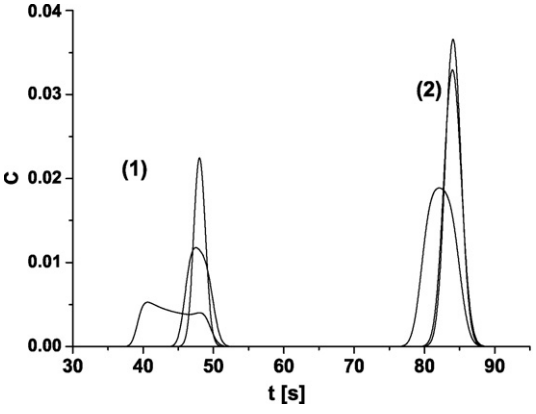

Fig. 5. Comparison between peak profiles calculated under conditions (a)–(c)—see text. The first group of peaks was calculated for F_v = 1.5 and the second for F_v = 0.8.

5. Conclusions

The numerical solutions of the ED, the TD, or the POR models of the mass balance equation coupled with the original model of heat transfer in VHPLC columns that was previously developed [21,22] are all in excellent agreement. This agreement was observed for a range of column inlet pressures between about 40 bar up to 1000 bar, which means that it is observed for columns packed with sub-2 μm particles that are operated under such experimental conditions that their efficiency is either very high or very low. The only requirement to achieve this agreement is that the apparent axial dispersion or the effective overall mass transfer coefficients be calculated using Eqs. (10) or (14), respectively. Because the calculations are much faster with the ED model than with the TD model and especially with the POR model, the simplest ED model is recommended for the modeling of the VHPLC process.

The heat transfer model coupled with the ED model in the version discussed in this work provided an excellent agreement between experimental and theoretical profiles for a series experiments performed using water bath temperatures of 299, 310, and 329 K. To achieve this good degree of agreement, only one experimental parameter had to be calculated on the basis of only one experimental band profile recorded at each temperature. The model described to account for the consequences of thermal phenomena resulting in a thermally heterogeneous column enables the calculation of accurate elution profiles even when the column is placed in a temperature-controlled water bath, extreme condition that promote considerable efficiency losses and that are certainly not the recommended mode of operation for maximum column efficiency. It will work as well when the column is in a less drastic thermal environment.

The model of coupled heat and mass transfer that we proposed could be used for the calculation of the optimum separation conditions of column working in VHPLC conditions and used for semi-preparative applications.

Acknowledgments

This work was partially supported by grant N N204 002036 of the Polish Ministry of Science and Higher Education. Financial support from the European Social Fund, Polish National Budget, Podkarpackie Voivodship Budget (within Sectoral Operational Program Human Resources) “Wzmocnienie instytucjonalnego systemu wdrazania Regionalnej Strategii Innowacji w latach 2007-2013” is gratefully acknowledged.

References

[1] I. Halasz, R. Endele, J. Asshauer, J. Chromatogr. 112 (1975) 37.
[2] H. Poppe, J.C. Kraak, J.F. Huber, Chromatographia 14 (1981) 515.
[3] H.-J. Lin, C. Horvath, Chem. Eng. Sci. 56 (1981) 47.
[4] H. Poppe, J.C. Kraak, J. Chromatogr. 282 (1983) 399.
[5] T. Welsch, M. Schmid, J. Kutter, A. Kalman, J. Chromatogr. A 728 (1996) 299.
[6] A. Brandt, G. Mann, W. Arlt, J. Chromatogr. A 769 (1997) 109.
[7] O. Dapremont, G.B. Cox, M. Martin, P. Hilaireau, H. Colin, J. Chromatogr. A 796 (1998) 81.
[8] A. DeVilliers, H. Lauer, R. Szucs, S. Goodal, P. Sandra, J. Chromatogr. A1113 (2006) 84.
[9] D.T.T. Nguyen, D. Guillarme, S. Heinisch, M.P. Barrioulet, J.L. Rocca, S. Rudaz, J.L. Veuthey, J. Chromatogr. A 1113 (2006) 84.
[10] F. Gritti, G. Guiochon, J. Chromatogr. A 1131 (2006) 151.
[11] G. Desmet, J. Chromatogr. A 1116 (2006) 89.
[12] U.D. Neue, M. Kele, J. Chromatogr. A 1149 (2007) 236.
[13] F. Gritti, G. Guiochon, J. Chromatogr. A 1138 (2007) 141.
[14] F. Gritti, G. Guiochon, Anal. Chem. 80 (2008) 5009.
[15] F. Gritti, G. Guiochon, J. Chromatogr. A 1187 (2008) 165.
[16] K. Kaczmarski, F. Gritti, G. Guiochon, J. Chromatogr. A 1177 (2008) 92.
[17] F. Gritti, G. Guiochon, Anal. Chem. 80 (2008) 6488.
[18] F. Gritti, M. Martin, G. Guiochon, Anal. Chem. 81 (2009) 3365.
[19] M.M. Fallas, M.R. Hadley, D.V. McCalley, J. Chromatogr. A 1216 (2009) 3961.
[20] F. Gritti, G. Guiochon, J. Chromatogr. A 1216 (2009) 1353.
[21] K. Kaczmarski, J. Kostka, W. Zapała, G. Guiochon, J. Chromatogr. A 1216 (2009) 6560.
[22] K. Kaczmarski, F. Gritti, J. Kostka, G. Guiochon, J. Chromatogr. A 1216 (2009) 6575.
[23] K. Kaczmarski, D. Antos, H. Sajonz, P. Sajonz, G. Guiochon, J. Chromatogr. A 925 (2001) 1.
[24] D. Antos, K. Kaczmarski, W. Piatkowski, A. Seidel-Morgenstern, J. Chromatogr. A 1006 (2003) 61.
[25] G. Guiochon, A. Felinger, A.M. Katti, D. Shirazi, Fundamentals of Preparative and Nonlinear Chromatography, second ed., Elsevier, Amsterdam, 2006.
[26] R. Pfeffer, Ind. Eng. Chem. Fundam. 3 (1964) 380.

[27] E.J. Wilson, C.J. Geankoplis, Ind. Eng. Chem. Fundam. 5 (1966) 9.
[28] T. Kataoka, H. Yoshida, K. Ueyama, J. Chem. Eng. Jpn. 5 (1972) 132.
[29] K. Miyabe, M. Ando, N. Ando, G. Guiochon, J. Chromatogr. A 1210 (2008) 60.
[30] D. Gunn, Chem. Eng. Sci. 363 (1987) 42.
[31] C.Y. Wen, L.T. Fan, Models for Flow Systems and Chemical Reactors, Marcel Dekker Inc., New York, 1975, p. 137.
[32] E.G. Scheibel, Ind. Eng. Chem. 46 (1954) 2007.
[33] K. Miyabe, N. Ando, G. Guiochon, J. Chromatogr. A 1216 (2009) 4377.
[34] D. Horne, J.H. Knox, L. McLaren, Sep. Sci. 1 (1966) 531.
[35] J.H. Knox, G.R. Laird, P.A. Raven, J. Chromatogr. 122 (1976) 129.
[36] K. Kaczmarski, G. Storti, M. Mazzotti, M. Morbidelli, Comput. Chem. Eng. 21 (1997) 641.
[37] P.N. Brown, A.C. Hindmarsh, G.D. Byrne, available at http://www.netlib.org.
[38] F. Gritti, Y. Kazakevich, G. Guiochon, J. Chromatogr. A 1161 (2007) 157.